

Structural and Magnetic Modification in Al₂O₃-CoO Nanocrystalline with CoO Dopant Concentrations

Seema¹, Sunita Dahiya², Rajesh Sharma^{3*}

¹Research Scholar, Baba Mastnath University, Rohtak-124001, India

²Faculty in Physics, Baba Mastnath University, Rohtak-124001, India

³Faculty in Physics, MNS Govt. College, Bhiwani - 127021, India

#Corresponding Author- rkkaushik06@gmail.com

ABSTRACT

The property of material changes with increase of surface atoms and especially proved contrasting behavior at the scale of nanometer. Among other metal Oxides Aluminium Oxide (Al₂O₃) have knee applications in the field of liquid crystal displays, high-temperature resistant materials, corrosive resistant materials, green pigment etc. The CoO (cobaltous oxide) have advance applications in the area of MRI and alloy formations. In present work, the CoO doped Al₂O₃ were synthesized by the Micro-wave irradiated chemical co-precipitation advance synthesis techniques. The ignited stuffs at 600°C/ 2hrs of various concentrations were characterized by the use of VSM, XRD, SEM, FTIR and the ionic TEM tools. The XRD results reveals that the grain size of newly calcined nanocomposites rises with rise of CoO concentration 5%, 10% and 20% and may be due to larger radii of Co²⁺ (Cobaltous ion) then Aluminium. The FTIR Spectra of the ignited nano stuffs of CoO doped Al₂O₃ containing were found at wave number position sharp alps(peaks) inspected at 837cm⁻¹ was due to Co-O-Co formation and 516cm⁻¹, 494 cm⁻¹ were due to O-Al-O vibration of Alumina molecules. The Perusal of TEM images exhibit that the size of all ignited CoO doped Al₂O₃ nanoparticulates lies in a confine of 31 nm to 42 nm and the intermediate fleck size is observed as 34 nm. The Perusal of scanning of sample through FESEM image is exhibiting that the flecks are polycrystalline in the formation, cluttered in style and spherical in contour.

Keywords: Alumina nanocrystalline, XRD, FESEM, FTIR, TEM and VSM etc.

INTRODUCTION

Nanoscience focuses on understanding and manipulating materials at an extremely small scale, typically between one and one hundred nanometers. At this nanoscale, particles and materials exhibit unique properties that differ significantly from their larger counterparts. Alumina, or aluminum oxide (Al₂O₃), is a hard, durable material widely used in science and industry. It's highly resistant to heat and corrosion, making it perfect for high-temperature applications, such as lining furnaces and kilns. In electronics, alumina is a common substrate for microchips due to its electrical insulation. It's also used in medical implants and as an abrasive in polishing because of its toughness.

Cobalt is a hard, magnetic metal with a silvery-blue color. It's resistant to wear, corrosion, and high temperatures, making it valuable in many scientific applications. Cobalt is commonly used in rechargeable batteries, like those in electric vehicles, due to its ability to store energy well. In medicine, cobalt-60, a radioactive isotope, is used in cancer treatment for radiotherapy. It's also an essential part of superalloys, which are materials that withstand extreme heat and are used in jet engines and turbines.

In present work, the researcher synthesis the various Co (5%, 10%, 20%) doped alumina nanoparticulates via microwave irradiated chemical co-precipitation techniques and resulted samples were calcined at 600°/2hrs. The purpose of researcher is to analysis structural and magnetic property.

Synthesis Techniques

The chemicals/salts used in present work have highly pure in nature and not be purified at laboratory scale. The appropriate molar concentration of Al(NO₃)₃·9H₂O(s) and Co(NO₃)₃·9H₂O(s) were taken as source of Alumina and Cobaltous and dissolved in 100ml doubly de-ionized water. The sparkle blackish solution were in formation and intensity of black color increase with Co²⁺ ion concentration in solution. The (NH₄OH) ammonia solution were taken as precipitate agent and added drop wise to rise the ph of solution and ph≥8.0 the disassociation of ion take place. The blackish color precipitate were kept for 24 Hrs in lab for aging process/stabilization. Then precipitate were filtered and washed with ethanol and double de-ionized water multi times to remove the contamination of nitrate present in samples.

The resulted samples were irradiated by microwave at temperature 125°C for 15 minutes 2 sitting to minimize the water contamination. Thereafter, the dried cake were calcined at 600°/2hrs in electric furnace and crushed the material to become fine powdered samples were examined through XRD, VSM, FESEM and HRTEM tools and results of respective study shown in coming sections.

CHARACTERIZATION OUTCOMES AND DISCUSSION

X-ray Diffraction Investigations

The X-rays were used to scan the diffracted peak of samples in range of $2\theta \approx 10^\circ$ to 80° with scan rate 57 min/sec. The presual of graph shows that major Alps(peaks) for Al_2O_3 nano-flecks with 5% dopant concentration at $200^\circ C$ were reported to be at $2\theta \sim 7.89^\circ, 37.17^\circ, 43.17^\circ, 62.55^\circ$ and 74.85° and at 78.82° as per the JCPDS file no. 072-3533. The Alps(peaks) with 10% dopant concentration were outlined at $37.06^\circ, 43.03^\circ$ and $47.84^\circ, 47.37^\circ, 62.38^\circ, 73.32^\circ, 78.66^\circ$. The peaks with Cobaltous Oxide doped Aluminium Oxide (20%) nano-sized stuff reported at $2\theta \sim 37.17^\circ, 43.016^\circ, 47.83^\circ, 62.55^\circ, 74.93^\circ$ and at 78.66° .

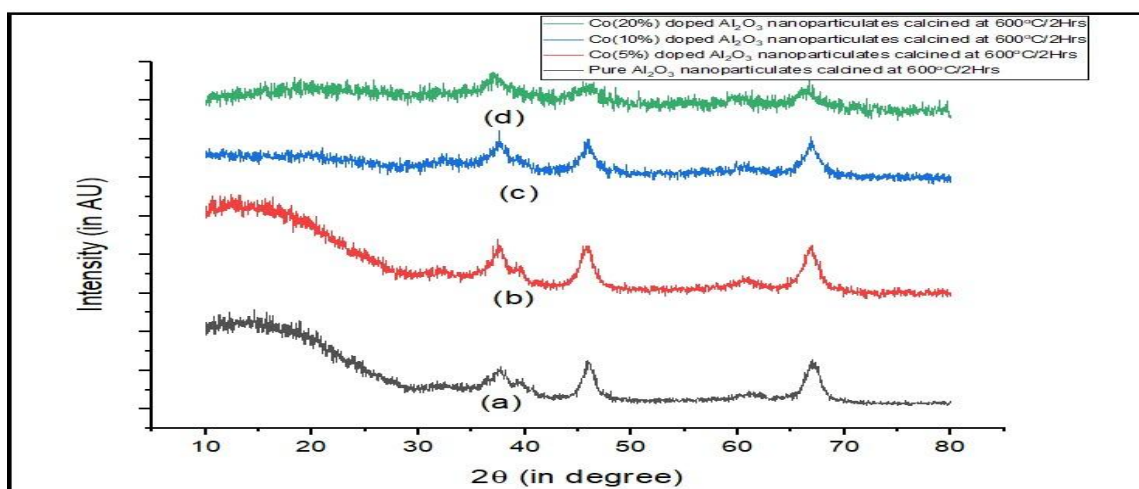


Figure -1. XRD graph of Cobaltous Oxide (CoO) doped Aluminium Oxide (Al_2O_3) ((5%, 10%, 20%) nano-sized stuff ignited at $600^\circ C$ for 2 hours

To estimate the size of the crystals, the breadth (β) of the most intense XRD peak was used in Debye-Scherrer's equation. This method allowed researchers to calculate the crystal sizes (D). The values of β and the corresponding crystal sizes (D) are displayed in Table 1. By using XRD data and Debye-Scherrer's equation, the size of the crystalline particles was systematically determined.

Table-1. XRD facts of CoO nano-flecks and CoO doped Al_2O_3 nano-sized stuff ignited at $600^\circ C$ with various dopant concentration

Sr. No.	Title of specimen	period of calcinations	Spot of uttermost intense Alp (in degree)	Measure of FWHM or(β) (in radian)	Grain size
1.	CoO doped Al_2O_3 (5%) NCs	2 hours	46.17	0.423	36.06 nm
2.	CoO doped Al_2O_3 (10%) NCs	2 hours	46.03	0.436	34.17 nm
3.	CoO doped Al_2O_3 (20%) NCs	2 hours	46.01	0.457	33.10 nm
4.	Pure Al_2O_3	2 hours	45.87	0.35	42.56 nm

From above table it can be investigated that the crystallite size goes on decrease with increase the doped concentration due to decrease ionic radii of cobalt ions.

FTIR Investigations

The FTIR were used to confirm the functional group of samples. The FTIR electromagnetic spectrum of synthesized specimen of CoO(5%, 10% and 20%) doped Al_2O_3 nano-sized stuff ignited at 600°C are exhibited for a fixed time duration of 2hrs was performed using a Perkin Elmer instrument at Punjab University located at Chandigarh. The graphical representation of the obtained data is explored in the figure-2.

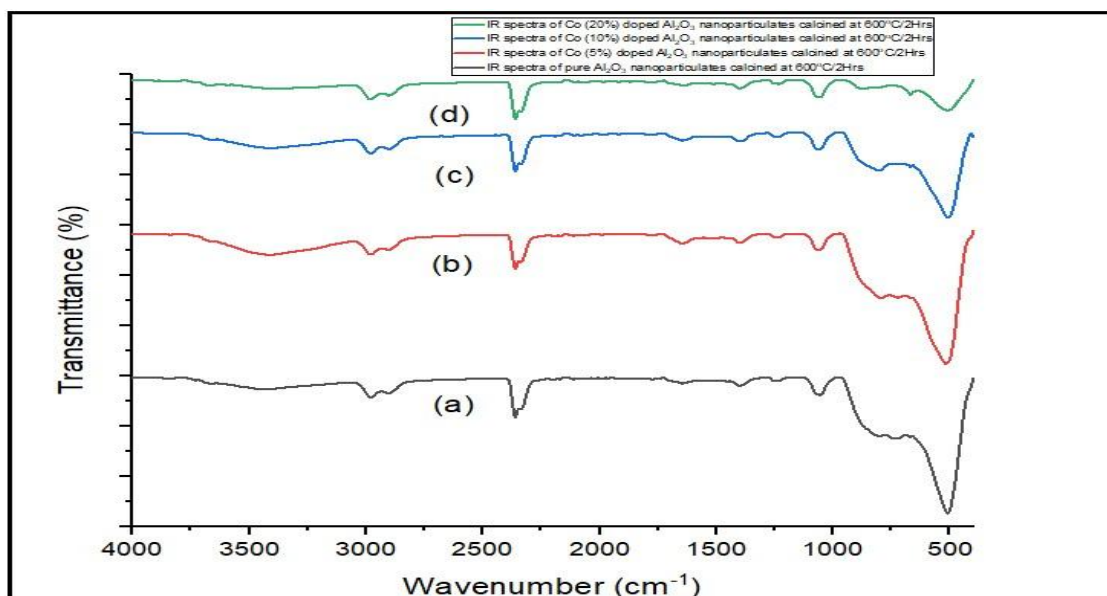


Figure-2. FTIR Spectra of Cobaltous Oxide doped Al_2O_3 nano-sized stuff with various molar concentrations ignited at 600°C for 2 hours (a) $\text{CoO} - \text{Al}_2\text{O}_3$ (5%)(b) $\text{CoO} - \text{Al}_2\text{O}_3$ (10%) (c) $\text{Co} - \text{Al}_2\text{O}_3$ (20%) nano-sized stuff

The perusal of graph shows that various peaks position of various kind of peak such as Broad band, solder, sharp, minute were observed in spectrograph. The observed peak position was 3402cm^{-1} , 2318cm^{-1} , 2337cm^{-1} , 2330cm^{-1} , 837cm^{-1} , 516cm^{-1} .

The peak observed at 3402cm^{-1} , 2330cm^{-1} , 1546cm^{-1} were maybe accredited by presence of water in atmosphere. Whereas sharp alps(peaks) inspected at 837cm^{-1} was due to Co-O-Co formation and 516cm^{-1} , 494cm^{-1} were due to oxide formation of metal i.e., the Alps(peaks) were attributing the Co-O-Co vibrations and these Alps(peaks) and therefore, confirmed the presence of CoO in Al_2O_3 nano-sized stuff.

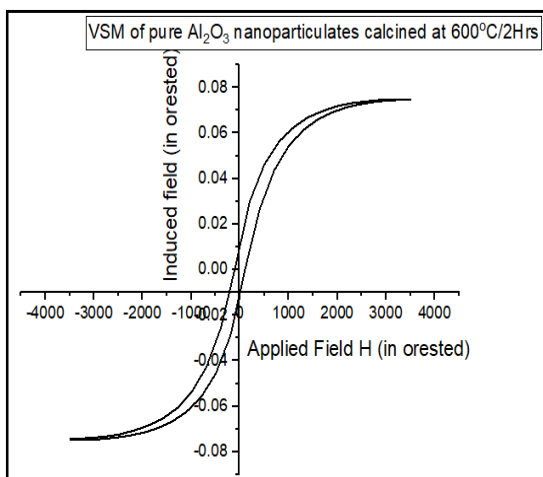
The X-ray powder diffraction (XRD) analysis of the synthesized Alumina nanoparticles revealed several characteristic peaks, indicating the presence of various functional groups. At peak positions 516cm^{-1} and 837cm^{-1} , Al-O-Al and Co-O-Co vibrations were identified.

A peak at 1300cm^{-1} corresponds to Co-O-Al bonding. Additionally, peaks at 1546cm^{-1} , 2330cm^{-1} , and 3402cm^{-1} indicate the presence of -OH groups. These -OH group vibrations are due to water molecules present in the atmosphere, which interact with the nanoparticles. This detailed analysis helps in understanding the chemical structure and bonding of the synthesized Alumina nanoparticles.

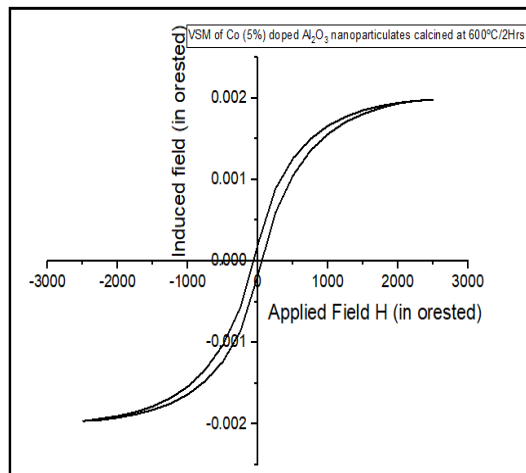
Vibrating Sample Magnetometer

Vibrating sample magnetometer is used to find out the magnetic property of the samples. In present work the various calcined samples of Cobalt (Co) 5%,10%,20% doped alumina nanocrystalline were studied through vsm tool and result were compare with pure alumina sampled calcined at 600°C for 2 hrs. The data received from lab CEERI Pilani were represented in various graph.

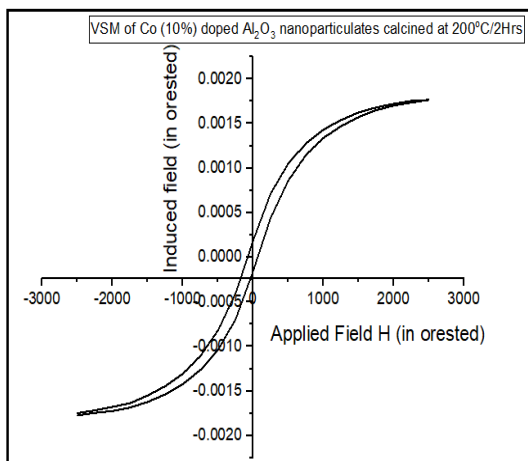
The preusal of graphically representation show that the particles are more or less ferromagnetic in nature with small hysteresis loss.



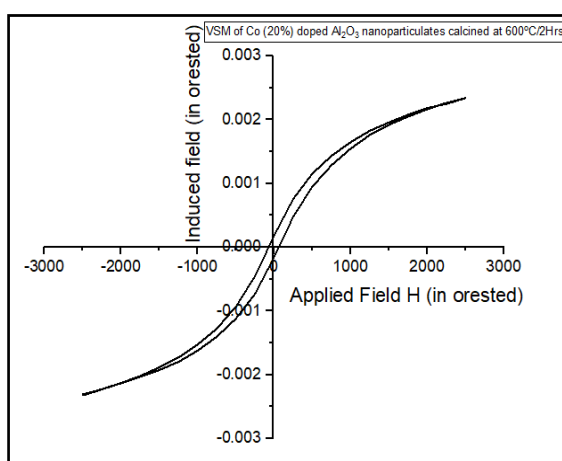
(a)



(b)



(c)



(d)

Table 2 Magnetic parametric data of pure Alumina and Co (5%, 10%, 20%) doped Alumina specimen calcined at 600°C for 2hrs.

Sr. No.	Sample Name	Saturation Magnetiz	Coercive Field (in Hc Oe)	Maximum Permeability (in 10^{-6})	Max. energy loss (in MGsOe)	Remanent magnetization (10^{-3} emu/g)
1	Pure Aluminaaaa	74.653	105.673	97.703	14.215	10.220
2	Co doped Al ₂ O ₃ 5%	1.974	60.329	3.047	7.490	185.95
3	Co doped Al ₂ O ₃ 10%	1.489	74.222	2.023	7.183	151.559
4	Co doped Al ₂ O ₃ 20%	2.333	65.687	2.549	7.713	167.569

VSM results reflects that saturation magnetization, coercive field, maximum permeability and maximum energy loss continuously reduce with increase of dopant concentration up to concentration of CoO 10% doped and their after slowly increase saturation magnetization, maximum permeability and maximum energy loss and continuously decrease coercive field at 20%. It might be due to localized magnetization effect in the crystal because of distortion occurred at higher concentration such as 20%.

FESEM images investigations

The scanning of sample through electron microscopy images of CoO doped Al₂O₃ nano-sized stuff ignited at 600 °C for 2 hours were more or less similar to typical scanning of sample through electron microscopy [225]. Micrograph of CoO doped Al₂O₃ (10%) nano-composites ignited at 600°C for 2 hours is exhibited in **Image 1**

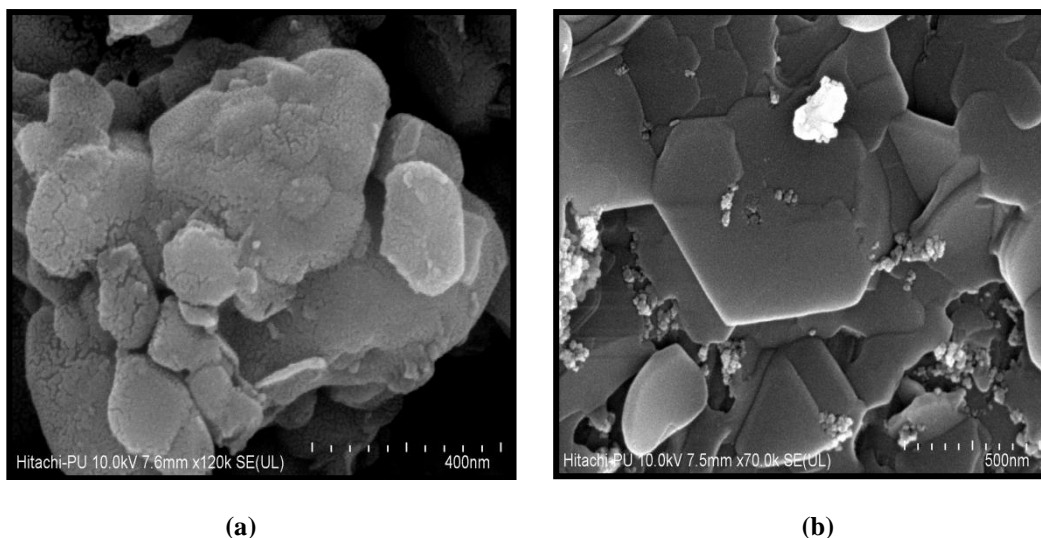


Figure-4: FESEM image of 10% pure Aluminium Oxide nanocrystalline calcined at temperature (a) 400°C (b) 600°C for fixed time interval of two hours.

Examination of Image exhibits that flecks are polycrystalline, cluttered in style and truncated spherical in contour.

High-Resolution Transmission Electron Microscope (HRTEM)

HRTEM studies of pure Aluminium Oxide nano-particulates which were ignited at 600°C ignition temperature for a fixed time period of 2 hours were done in CIL Lab, Punjab University, Chandigarh and the recorded images were illustrated in the figure below. TEM micro-graphs of CoO doped Al_2O_3 nano-composites with various concentrations (5%, 10%, 20%) ignited at 600°C for 2 hours are exhibited. The images of HRTEM illustrate that the size of prepared undoped Al_2O_3 nanocrystalline is less than 50nm and lies in the nano-regime.

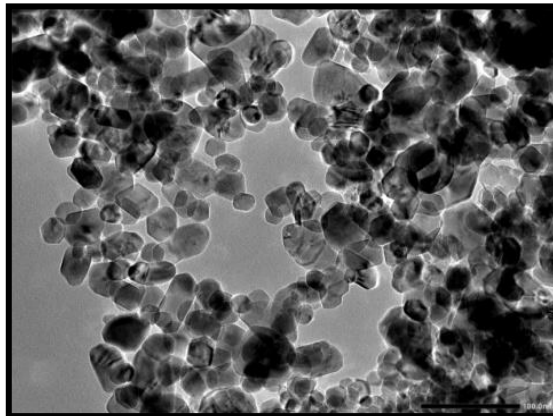


Figure-5: HRTEM images of CoO doped Al_2O_3 (10%) nano-sized stuff ignited at 600°C for 2 hours

Examination of the Image exhibits that diameter of the nano-sized stuff ranging from 23.01 to 42.56 nm and intermediate grain size estimated to be 34nm. The micrographs of TEM concluded that grain size results resemble with XRD results and clarified that grain size rises with doping molar concentration. From the micro-graph, it was inspected that the nano-fleck are polycrystalline kind and spherical in contour.

CONCLUSIONS

The Cobaltous doped Alumina nano-crystalline were successfully synthesized by advance chemical co-precipitation protocol and XRD results concluded that crystallite size increases with dopant concentration and composition ratio of α -alumina decrease with increase of calcinations temperature respectively.

The FESEM and HRTEM images insure the nanomaterial were 2-D nano-structured and thin film were in formations with different nano range sizes. The IR peaks emphasized that pure Alumina nanocrystalline were observed with different phase of occurrences. The IR results verify the XRD results.

REFERENCES

- [1]. Giribabu, G. et al. (2014) 'Structural, optical and magnetic properties of cobalt and aluminum co doped cds nanoparticles', *Materials Letters*, 126, pp. 119–122. doi:10.1016/j.matlet.2014.04.044.
- [2]. Rajesh Sharma et al. (2020) 'To study the structural properties of cobalt doped tin oxide nanostructured by using Williamson- and size-strain plot Hall methodology' doi.org/10.1016/j.matpr.2020.10.927,P1-6 ISSN2214-7853
- [3]. Dalvand, R. et al. (2020) 'MgO nano-sheets for adsorption of anionic dyes from aqueous solution: Equilibrium and Kinetics Studies', *Surfaces and Interfaces*, 21, p. 100722. doi:10.1016/j.surfin.2020.100722.
- [4]. Chu, H., Shi, W., et al. (2022) 'Feasibility of manufacturing self-compacting mortar with high elastic modulus by Al₂O₃ micro powder: A preliminary study', *Construction and Building Materials*, 340, p. 127736. doi:10.1016/j.conbuildmat.2022.127736.
- [5]. Choudhari, U. and Jagtap, S. (2022) 'Lanthanum doped tin oxide: Synthesis, characterization and application', *Materials Today: Proceedings*, 49, pp. 3325–3330. doi:10.1016/j.matpr.2021.01.129.
- [6]. Saneh Lataa et al. (2022) 'The Investigations of Change in Structural Parameters with Dopant Concentration of Iron (Fe) and Chromium (Cr) in Sn/Fe/Cr Nanostructured Materials' ISSN0973-4562Volume 17,Number 5(2022) pp. 475-479.
- [7]. Choudhari, K.S. et al. (2018) 'Photoluminescence enhancement and morphological properties of nanoporous anodic alumina prepared in oxalic acid with varying time and temperature', *Microporous and Mesoporous Materials*, 271, pp. 138–145. doi:10.1016/j.micromeso.2018.06.004.
- [8]. Chen, J. et al. (2018) 'The effect of Nano- γ Al₂O₃ additive on early hydration of calcium aluminate cement', *Construction and Building Materials*, 158, pp. 755–760. doi:10.1016/j.conbuildmat.2017.10.071
- [9]. CH, A., Rao K, V. and Chakra CH, S. (2021) 'Synthesis and characterization of zno/cuo nanocomposite for humidity sensor application', *Advanced Materials Proceedings*, 1(1), pp. 60–64. doi:10.5185/amp.2016/111.
- [10]. Abdulridha, G.R. and Hasan, Z.A. (2022) 'Study the effect doping (al₂o₃) nanoparticles on optical properties for PVA polymer', *NeuroQuantology*, 20(3), pp. 231–236. doi:10.14704/nq.2022.20.3.nq22065.
- [11]. Ali, M. et al. (2021) 'Biogenic synthesis, characterization and antibacterial potential evaluation of copper oxide nanoparticles against escherichia coli', *Nanoscale Research Letters*, 16(1). doi:10.1186/s11671-021-03605-z.
- [12]. Alrobei, H. et al. (2021) 'Adsorption of anionic dye on eco-friendly synthesised reduced graphene oxide anchored with lanthanum aluminate: Isotherms, kinetics and statistical error analysis', *Ceramics International*, 47(7), pp. 10322–10331. doi:10.1016/j.ceramint.2020.07.251.
- [13]. Alwan Resan, S. and Fadhel Essa, A. (2021) 'Preparation and study of the optical properties for polyaniline-al₂o₃ nanocomposite', *Materials Today: Proceedings*, 45, pp. 5819–5822. doi:10.1016/j.matpr.2021.03.182.
- [14]. Amika et al. (2022) 'Role of titanate-based perovskites in solar water splitting: An overview', *Journal of Physics: Conference Series*, 2267(1), p. 012016. doi:10.1088/1742-6596/2267/1/012016.
- [15]. Arnold, B. (2022) 'The Aluminium Oxide Family', *Rubies and Implants*, pp. 3–5. doi:10.1007/978-3-662-66116-1_2.
- [16]. Bidulská, J. et al. (2019) 'Different formation routes of pore structure in aluminum powder metallurgy alloy', *Materials*, 12(22), p. 3724. doi:10.3390/ma12223724.
- [17]. Brik, M.G. (2018) 'Ab-initio studies of the electronic and optical properties of al₂o₃:ti³⁺ laser crystals', *Physica B: Condensed Matter*, 532, pp. 178–183. doi:10.1016/j.physb.2017.02.032.
- [18]. Caballero-Calero, O. and Martín-González, M. (2020) '3D porous alumina: A controllable platform to tailor magnetic nanowires', *Magnetic Nano- and Microwires*, pp. 3–20. doi:10.1016/b978-0-08-102832-2.00001-3.
- [19]. Carrillo, C. et al. (2020) 'Synthesis and characterization of zinc oxide nanowires on aluminium oxide substrate', 2020 17th International Conference on Electrical Engineering, Computing Science and Automatic Control (CCE) [Preprint]. doi:10.1109/cce50788.2020.9299161.
- [20]. Carvajal, S. et al. (2019) 'Cerium oxide nanoparticles protect against oxidant injury and interfere with oxidative mediated kinase signaling in human-derived hepatocytes', *International Journal of Molecular Sciences*, 20(23), p. 5959. doi:10.3390/ijms20235959.
- [21]. Casals, E. et al. (2020) 'Cerium oxide nanoparticles: Cerium oxide nanoparticles: Advances in biodistribution, toxicity, and preclinical exploration (small 20/2020)', *Small*, 16(20), p. 2070111. doi:10.1002/sml.202070111.
- [22]. CH, A., Rao K, V. and Chakra CH, S. (2021) 'Synthesis and characterization of zno/cuo nanocomposite for humidity sensor application', *Advanced Materials Proceedings*, 1(1), pp. 60–64. doi:10.5185/amp.2016/111.
- [23]. Chahar, R. and Das Mukherji, M. (2022) 'Environmental applications of phytonanotechnology: A promise to sustainable future', *Phytonanotechnology*, pp. 141–159. doi:10.1007/978-981-19-4811-4_7.
- [24]. Chandla, N.K. et al. (2020) 'Experimental Analysis and mechanical characterization of AL 6061/alumina/bagasse ash hybrid reinforced metal matrix composite using vacuum-assisted stir casting method', *Journal of Composite Materials*, 54(27), pp. 4283–4297. doi:10.1177/0021998320929417.
- [25]. Chandrashekar, J.R., Annaiah, M.H. and Chandrashekar, R. (2021) 'Microstructure and mechanical properties of aluminum cast alloy A356 reinforced with dual-size B4C particles', *Frattura ed Integrità Strutturale*, 15(57), pp. 127–137. doi:10.3221/igf-esis.57.11.
- [26]. Chen, C.-H., Lin, Y.-C. and Yen, F.-S. (2021) 'Synthesis and characterization of conducting PANDB/ χ -al₂o₃ core-shell nanocomposites by in situ polymerization', *Polymers*, 13(16), p. 2787. doi:10.3390/polym13162787.

- [27]. Choudhari, K.S. et al. (2018) 'Influence of electrolyte composition on the photoluminescence and pore arrangement of nanoporous anodic alumina', *ECS Journal of Solid State Science and Technology*, 7(11). doi:10.1149/2.0081811jss.
- [28]. Choudhari, U. and Jagtap, S. (2022) 'Lanthanum doped tin oxide: Synthesis, characterization and application', *Materials Today: Proceedings*, 49, pp. 3325–3330. doi:10.1016/j.matpr.2021.01.129.
- [29]. Chu, H., Shi, W., et al. (2022) 'Feasibility of manufacturing self-compacting mortar with high elastic modulus by al₂o₃ micro powder: A preliminary study', *Construction and Building Materials*, 340, p. 127736. doi:10.1016/j.conbuildmat.2022.127736.
- [30]. Cuong, H.N. et al. (2022) 'New frontiers in the plant extract mediated biosynthesis of copper oxide (CuO) nanoparticles and their potential applications: A Review', *Environmental Research*, 203, p. 111858. doi:10.1016/j.envres.2021.111858.
- [31]. D.Simsek,I.Simsek,andd.ozyurek et al (2023).relationship between al₂o₃content and wear Available at: <https://www.degruyter.com/document/doi/10.1515/secm-2020-0017/pdf>
- [32]. Dalvand, R. et al. (2020) 'MgO nano-sheets for adsorption of anionic dyes from aqueous solution: Equilibrium and Kinetics Studies', *Surfaces and Interfaces*, 21, p. 100722. doi:10.1016/j.surfin.2020.100722.
- [33]. Dev Srivayas, P. and S. Charoo, M. (2018) 'Aluminum Metal Matrix Composites a review of reinforcement; mechanical and Tribological behavior', *International Journal of Engineering & Technology*, 7(2.4), p. 117. doi:10.14419/ijet.v7i2.4.13020.
- [34]. Dhabale, R.B. et al. (2023) 'Friction stir welding of dissimilar materials with reinforcement of copper particulates', *Key Engineering Materials*, 941, pp. 3–10. doi:10.4028/p-ltn695.